

# Lattice Index Theorem and Fractional Topological Charge

R. Höllwieser,<sup>1</sup> M. Faber,<sup>1</sup> and U.M. Heller<sup>2</sup>

<sup>1</sup>*Atomic Institute, Vienna University of Technology,  
Wiedner Hauptstr. 8-10, A-1040 Vienna, Austria*

<sup>2</sup>*American Physical Society, One Research Road, Ridge, NY 11961, USA*

(Dated: October 17, 2018)

We study topological properties of classical spherical center vortices with the low-lying eigenmodes of the Dirac operator in the fundamental and adjoint representations using both the overlap and asqtad staggered fermion formulations. In particular we address the puzzle raised in a previous work of our group [Phys. Rev. D 77, 14515 (2008)], where we found a violation of the lattice index theorem with the overlap Dirac operator in the fundamental representation even for “admissible” gauge fields. Here we confirm the discrepancy between the topological charge and the index of the Dirac operator also for asqtad staggered fermions and the adjoint representation. Numerically, the discrepancy equals the sum of the winding numbers of the spheres when they are regarded as maps  $\mathbb{R}^3 \cup \{\infty\} \rightarrow SU(2)$ . Furthermore we find some evidence for fractional topological charge during cooling the spherical center vortex on a  $40^3 \times 2$  lattice. The object with topological charge  $Q = 1/2$  we identify as a Dirac monopole with a gauge field fading away at large distances. Therefore even for periodic boundary conditions it does not need an antimonopole.

## I. INTRODUCTION

Topological models have been introduced to explain quark confinement in non-abelian gauge theories. There are good reasons to believe that a force strong enough to confine quarks must also break chiral symmetry spontaneously [1]. The center vortex model [2–7] seems to be the most promising candidate to explain both phenomena. Center vortices, quantized magnetic flux lines, compress the gluonic flux into tubes and cause a linearly rising potential at large separations. Numerical simulations have indicated that vortices could also account for phenomena related to chiral symmetry, such as causing topological charge fluctuations and spontaneous chiral symmetry breaking (SCSB) [8–11]. These non-perturbative features of the QCD vacuum are intimately linked to the properties of the low-lying spectrum of the Dirac operator. In Ref. [12] we found strong correlations between the center vortices and the density distribution of low-lying Dirac eigenmodes. We showed that even center-projected lattice configurations give rise to a spectral density of near-zero modes, which by the Banks-Casher relation [13] is proportional to the chiral condensate, the order parameter for SCSB. Another relation between fermions and topology is given by the Atiyah-Singer index theorem [14–17]. It states that the topological charge of a gauge field configuration equals the index of the Dirac operator in this gauge field background. In Ref. [18] we investigated the lattice index theorem and the localization of the zeromodes for thick classical center vortices. For nonorientable spherical vortices, the index of the overlap Dirac operator turned out to differ from the topological charge. This may be related to the fact that even in Landau gauge some links of this configuration are close to the nontrivial center elements.

In this paper, we work with thick spherical vortices in  $SU(2)$  lattice gauge theory and extend our analysis of the topological charge and the lattice index theorem.

In Sec. II we re-introduce the construction of a spherical vortex and report on our calculations with the overlap Dirac operator. After analyzing the response of (improved) staggered fermions to the topological background of the gauge field we investigate in Sec. III the localization of asqtad staggered zeromodes with respect to the position of the thick vortices and find the same discrepancy for the topological charge determined by different methods. We then examine the index theorem for adjoint fermions in Sec. IV and discuss the role of adjoint fermions with respect to fractional topological charge in Sec. V. We find an interesting configuration giving topological charge one half which we analyze in Sec. VI in more detail. We end with our conclusions.

## II. SPHERICAL CENTER VORTICES AND DIRAC ZERO MODES

The nonorientable spherical vortex of radius  $R$  and thickness  $\Delta$  is constructed with the following links:

$$U_\mu(x_\nu) = \begin{cases} \exp(i\alpha(|\vec{r} - \vec{r}_0|)\vec{n} \cdot \vec{\sigma}) & t = 1, \mu = 4 \\ \mathbb{1} & \text{elsewhere} \end{cases} \quad (2.1)$$

$$\text{with } \vec{n}(\vec{r}, t) = \frac{\vec{r} - \vec{r}_0}{|\vec{r} - \vec{r}_0|}, \quad (2.2)$$

where  $\vec{r}$  is the spatial part of  $x_\nu$  and the profile function  $\alpha$  is either one of  $\alpha_+, \alpha_-$ , which are defined by

$$\alpha_+(r) = \begin{cases} 0 & r < R - \frac{\Delta}{2} \\ \frac{\pi}{2} \left(1 - \frac{r-R}{\frac{\Delta}{2}}\right) & R - \frac{\Delta}{2} < r < R + \frac{\Delta}{2} \\ \pi & R + \frac{\Delta}{2} < r \end{cases}, \quad (2.3)$$

$$\alpha_-(r) = \begin{cases} \pi & r < R - \frac{\Delta}{2} \\ \frac{\pi}{2} \left(1 + \frac{r-R}{\frac{\Delta}{2}}\right) & R - \frac{\Delta}{2} < r < R + \frac{\Delta}{2} \\ 0 & R + \frac{\Delta}{2} < r \end{cases}. \quad (2.4)$$

This means that all links are equal to  $\mathbb{1}$  except for the  $t$ -links in a single time-slice at fixed  $t = 1$ . The phase changes from 0 to  $\pi$  from inside to outside (or vice versa). The graph of  $\alpha_-(r)$  for a  $40^3 \times N_t$ -lattice is plotted in Fig. 2 in [18], giving a hedgehog-like configuration, without any intersections and hence no topological charge. Since only links in the time direction are different from  $\mathbb{1}$ , the topological charge determined from any lattice version of  $F\bar{F}$  vanishes for this spherical vortex configuration. We shall refer to such determinations as topological charge in the rest of this paper.

However, we find a discrepancy to the index of the overlap Dirac operator [17, 19, 20]. According to the Atiyah-Singer index theorem the topological charge is related to the index by  $\text{ind } D[A] = n_- - n_+ = Q$  where  $n_-$  and  $n_+$  are the number of left- and right-handed zero modes of the Dirac operator [14–16]. For the spherical vortex configuration, Eq. (2.2), we obtain a nonzero index.

The lattice version of the index theorem is only valid as long as the gauge field is smooth enough and satisfies a so-called “admissibility” condition. This condition assures that  $H_L^+$  has no zero eigenvalues so that the sign function in the definition of the overlap Dirac operator is well defined. It requires that the plaquette values  $U_{\mu\nu}$  are bounded close to  $\mathbb{1}$ , the value for very smooth gauge fields. A sufficient, but not necessary bound for the “admissibility” of the gauge field is  $\text{tr}(\mathbb{1} - U_{\mu\nu}) < 0.03$  [21–23]

On a  $40^3 \times N_t$ -lattice the traces of the plaquettes for the spherical vortex, Eq. (2.2), deviate only by a maximum of 1.5% from trivial plaquettes, satisfying the “admissibility” condition. Nevertheless, the index of the overlap operator is nonzero,  $\text{ind } D = \mp 1$ , for  $\alpha_{\pm}$ .

To try to understand the discrepancy we apply standard cooling to the spherical vortex configuration. For many cooling steps, the index of the overlap Dirac operator does not change, but the topological charge quickly rises close to  $\mp 1$  for  $\alpha_{\pm}$  while the action  $S$  reaches a (nonzero) plateau, as shown in Fig. 1 for a  $40^3 \times 4$  lattice. So, the index of the overlap Dirac operator agrees with the topological charge after some cooling, but not on the original vortex configuration.

### III. TOPOLOGY AND STAGGERED FERMIONS

Staggered fermions don’t have exact zero modes, but a separation between “would-be” zero modes and nonchiral modes is observed for improved staggered quark actions [24]. These results shall be verified first, by comparing standard and asqtad improved staggered fermions and by using the HYP (hypercubic blocking) smearing algorithm [25]. The results are shown in Fig. 2, presenting the first twenty eigenmodes of thirty configurations, generated by lattice Monte Carlo simulation of the tadpole improved Lüscher-Weisz pure-gauge action at coupling  $\beta_{LW} = 3.7$  (lattice spacing  $a \approx 0.09$  fm). We chose a fairly small lattice spacing to keep lattice effects as small

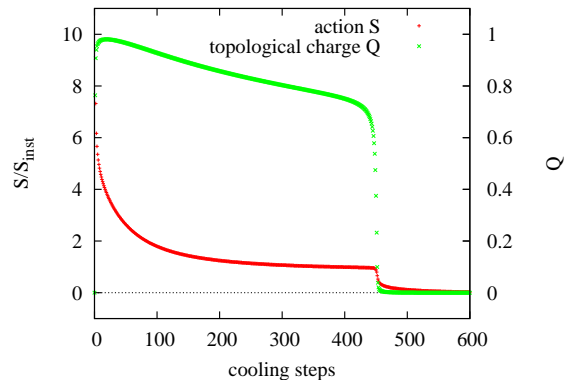


FIG. 1. Cooling of a spherical vortex on a  $40^3 \times 4$  lattice. The topological charge rises from zero to close to one for  $\alpha = \alpha_-$  (right scale) while the action  $S$  (in units of the one-instanton action  $S_{\text{inst}}$ ) reaches a plateau (left scale).

as practicable. The eigenvalues are plotted against the chirality (pseudoscalar density) of the modes, which for staggered fermions is determined by  $\langle \Psi \Gamma_5 \Psi \rangle$ , where  $\Gamma_5$  corresponds to a displacement along the diagonal of a hypercube. To ensure gauge invariance the product includes gauge field multiplications along all shortest paths connecting opposite corners of the hypercube. Comparing standard (red + symbols) and asqtad improved (green x symbols) staggered fermions, a slight improvement is observed for the latter: “would-be” zero modes show a higher chirality (up to 0.5) and eigenvalues are “closer” to zero. But for these still rather rough configurations it seems hard to really identify the would-be zero modes reliably. To make the configurations smoother, while retaining topological fluctuations, we applied five steps of HYP-smearing. Then the chirality of the would-be zero modes gets well defined and the eigenvalues get close to zero. On these smoothed configurations there is no big difference between standard (blue \* symbols) and asqtad improved (magenta □ symbols) fermions anymore.

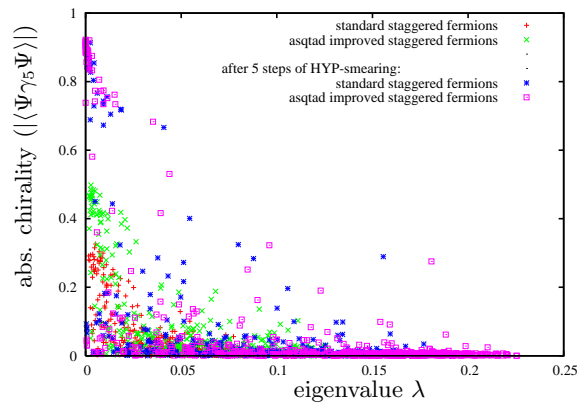


FIG. 2. The first twenty eigenmodes of thirty Monte Carlo configurations on a  $20^4$  lattice, for standard and asqtad staggered fermions on the original and HYP-smearred gauge fields, with antiperiodic boundary conditions.

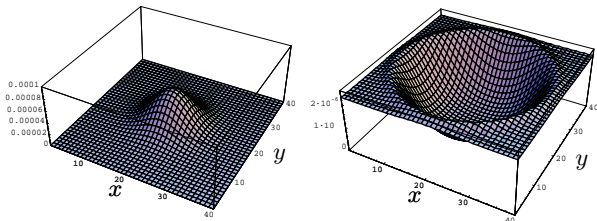


FIG. 3. Scalar densities of asqtad staggered zeromode of positive chirality for the positive ( $\alpha_+$ , left) and negative chirality for the negative ( $\alpha_-$ , right) spherical vortex in a time slice of a  $40^3 \times 8$  lattice, with antiperiodic boundary conditions.

These results promise that one should be able to identify zeromodes reliably on smooth configurations, such as the above examples of spherical vortices. The asqtad staggered modes were calculated for a positive and a negative non-orientable spherical vortex made up of time links in a single time slice of a  $40^3 \times 8$  lattice. Due to charge conjugation, staggered eigenmodes are doubly degenerated but according to the index theorem ( $\text{ind } D[A] = n_- - n_+ = 2Q$ ) we get exactly the same topological charge as the overlap Dirac operator. The scalar densities of the would-be zeromodes for both types of spherical vortices show a distribution (Fig. 3) that looks very similar to their overlap counterparts (see [18]).

#### IV. INDEX THEOREM AND ADJOINT FERMIONS

It is also interesting to study the correlation of the number of zeromodes and the topological charge for fermions in the adjoint representation, as discussed at recent lattice conferences (see *e.g.*, [26]). The index of the massless Dirac operator in the adjoint representation of the  $SU(N)$  gauge group in a background field of topological charge  $Q$  is equal to  $2NQ$  [27]. We test the lattice index theorem for overlap and asqtad staggered fermions in the adjoint color representation on the spherical vortex configurations, Eq. (2.1). Since the fermion is in the real representation, the spectrum of the adjoint Dirac operator is doubly degenerate. Therefore, the index can only be even valued. It will be interesting whether we find all possible even values or only multiples of four, resulting in a gauge field background made up of classical instantons.

In Table I the number of positive and negative overlap and staggered zeromodes in the fundamental and adjoint representation for periodic and antiperiodic boundary conditions on positive and negative spherical vortex configurations on different lattice sizes are summarized. Concerning this table we like to mention two issues. All investigated fermion representations equally violate the lattice index theorem for these special configurations: the index is nonzero while the topological charge vanishes. Further, in some cases, indicated in bold, the adjoint index is not a multiple of four, as will be discussed in the

next sections.

To study the above mentioned violation, we consider the homotopy of the above spherical vortex configurations, Eq. (2.1). The  $t$ -links of these spherical vortices fix the holonomy of the time-like loops, defining a map  $U_t(\vec{x}, t=1)$  from the  $xyz$ -hyperplane at  $t=1$  to  $SU(2)$ . Because of the periodic boundary conditions, the time-slice has the topology of a 3-torus. But, actually, we can identify all points in the exterior of the 3 dimensional sphere since the links there are trivial. Thus the topology of the time-slice is  $\mathbb{R}^3 \cup \{\infty\}$  which is homeomorphic to  $S^3$ . A map  $S^3 \rightarrow SU(2)$  is characterised by a winding number

$$\mathcal{N} = -\frac{1}{24\pi^2} \int d^3x \epsilon_{ijk} \text{tr}[(U^\dagger \partial_i U)(U^\dagger \partial_j U)(U^\dagger \partial_k U)], \quad (4.1)$$

resulting in  $\mathcal{N} = -1$  for positive and  $\mathcal{N} = +1$  for negative spherical vortices. With this assignment the index of the Dirac operator and the topological charge after cooling coincide with this winding number  $\mathcal{N}$ . Obviously such windings, given by the holonomy of the time-like loops of the spherical vortex, influence the index theorem [28, 29].

#### negative spherical vortex

	fundamental:		adjoint:						
	overlap:	asqtad:	overlap:	asqtad:					
lattice:	pbc:	apbc:	pbc:	apbc:	pbc:	apbc:	pbc:	apbc:	
$8^4$ :	3+4-	0+1-	6+8-	0+2-	4+6-	0+2-	8+12-	0+4-	
$12^4$ :	3+4-	0+1-	6+8-	0+2-	4+6-	0+2-	8+12-	0+4-	
$16^4$ :	3+4-	0+1-	6+8-	0+2-	4+8-	0+4-	8+16-	0+8-	
$20^4$ :	3+4-	0+1-	6+8-	0+2-	4+8-	0+4-	8+16-	0+8-	
$40^3 \times 2$ :	3+4-	0+1-	6+8-	0+2-	4+8-	0+4-	8+16-	0+8-	
cooled:	3+4-	0+1-	6+8-	0+2-	4+6-	0+2-	8+12-	0+4-	
$40^3 \times 4$ :	3+4-	0+1-	6+8-	0+2-	4+8-	0+4-	8+16-	0+8-	

#### positive spherical vortex

	fundamental:		adjoint:						
	overlap:	asqtad:	overlap:	asqtad:					
lattice:	pbc:	apbc:	pbc:	apbc:	pbc:	apbc:	pbc:	apbc:	
$8^4$ :	1+0-	4+3-	2+0-	8+6-	<b>6+4-</b>	<b>2+0-</b>	<b>12+8-</b>	<b>4+0-</b>	
$12^4$ :	1+0-	4+3-	2+0-	8+6-	<b>6+4-</b>	<b>2+0-</b>	<b>12+8-</b>	<b>4+0-</b>	
$16^4$ :	1+0-	4+3-	2+0-	8+6-	8+4-	4+0-	16+8-	8+0-	
$20^4$ :	1+0-	4+3-	2+0-	8+6-	8+4-	4+0-	16+8-	8+0-	
$40^3 \times 2$ :	1+0-	4+3-	2+0-	8+6-	8+4-	4+0-	16+8-	8+0-	
cooled:	1+0-	4+3-	2+0-	8+6-	<b>6+4-</b>	<b>2+0-</b>	<b>12+8-</b>	<b>4+0-</b>	
$40^3 \times 4$ :	1+0-	4+3-	2+0-	8+6-	8+4-	4+0-	16+8-	8+0-	

TABLE I. Number of positive and negative overlap and staggered zeromodes in the fundamental and adjoint representation for periodic and antiperiodic boundary conditions on positive and negative spherical vortices on different lattice sizes. Numbers which indicate half-integer topological charge are printed in bold.

## V. ADJOINT ZEROMODES AND FRACTIONAL TOPOLOGICAL CHARGE

Classical instantons carry an integer topological charge. Thus, in case of a fermion in the fundamental representation of  $SU(2)$  there is exactly one zero mode for a one-instanton configuration. Now, if the actual constituents of the QCD vacuum had topological charge  $Q = 1/2$ , no zero mode would be produced. However, for adjoint fermions configurations with topological charge  $Q = 1/2$  are able to create a zero mode. Edwards et al. presented in [27] some evidence for fractional topological charge on the lattice. García-Pérez et al. [26], however, associated this to lattice artefacts, *i.e.*, topological objects of size of the order of the lattice spacing. For comparison we repeat the calculations with Monte Carlo configurations on  $12^4$  lattices for overlap and  $16^4$  lattices for asqtad staggered fermions. In the first case we find for five out of twenty configurations a number of overlap zero modes which is not a multiple of four, *i.e.*, 2, 6, 6, 10, 10. For adjoint asqtad staggered fermions multiples of eight are expected, since staggered fermions have a doubly degenerate eigenvalue spectrum. Nevertheless we even find a couple of configurations with one or two “zero modes”, but of course it is not clear whether all these low-lying modes are would-be zero modes or whether all would-be zero modes were identified.

However, the measurements with adjoint fermions on the classical spherical vortices also show fractional topological charge for small lattice sizes, see Table I. Very interesting is the case of the cooled  $40^3 \times 2$  lattice configuration, which will be discussed next.

## VI. COOLING OF VORTEX CONFIGURATIONS

During cooling of a spherical vortex on a  $40^3 \times 2$  lattice we find evidence for fractional topological charge as shown in Fig. 4. It exhibits a second “plateau” for the topological charge with  $Q \approx 1/2$  between cooling steps 100 and 130. We analyzed this configuration with adjoint eigenmodes, which indeed measure fractional topological charge, as seen in Table I. The spherical vortex contracts during cooling as shown in Fig. 5. After 78 cooling steps the vortex structure vanishes. In the maximal abelian gauge one can identify a monopole-antimonopole ring after projection which again contracts during cooling and disappears after 91 cooling steps, see Fig. 6. In the interesting region with topological charge  $Q = 1/2$  (at cooling step 120), the action and topological charge densities concentrate in the center of the spacial volumes and the gauge field at the lattice boundary is trivial. Landau gauge yields a very symmetric configuration, a static, singular monopole without an antimonopole. In Landau gauge both time slices are exactly the same and all time-like plaquettes are trivial. The central cube in every time-slice is a non-abelian representation [30, 31] of a Dirac monopole, see also Fig. 9. Its six plaquettes

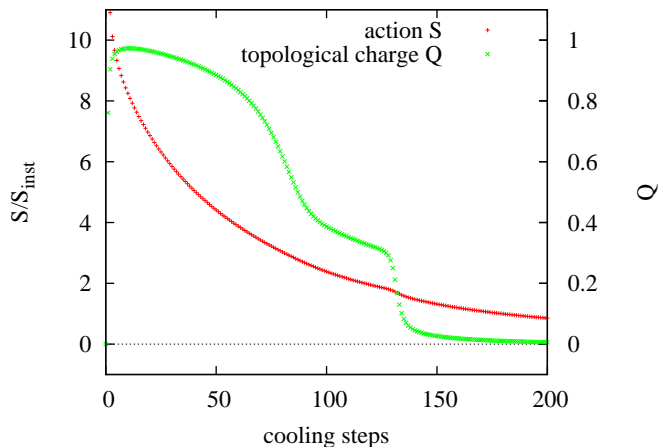


FIG. 4. Cooling of a spherical vortex with  $\alpha = \alpha_-$  on a  $40^3 \times 2$  lattice. While the action  $S$  (in units of the one-instanton action  $S_{\text{inst}}$ ) decreases slowly (left scale), the topological charge first rises from zero to close to one (right scale), then decreases to an intermediate plateau of  $Q \approx 0.4$  before it vanishes.

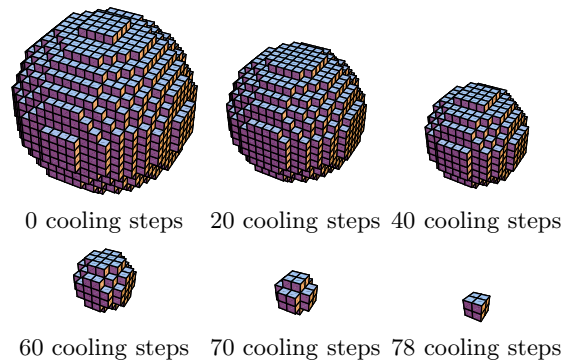


FIG. 5. Cooling of a spherical vortex on a  $40^3 \times 2$  lattices. The vortex shrinks and vanishes after 78 cooling steps.

correspond to rotations by  $2\pi/3$  in the fundamental representation of  $SU(2)$ . In the color frame of the corner with the smallest coordinate values the plaquette color vectors, parallel-transported according to Fig. 2 in [32], point in the  $(-1, -1, -1)$ -direction. Hence, the six plaquettes sum up to a total rotation of  $4\pi$  in agreement with the non-abelian lattice Bianchi identity, which states that the product of plaquette rotations in appropriate order results in the unit matrix. Nevertheless the magnetic flux out of the cube is nonvanishing [32].

In the  $U(1)$  representation in color direction  $(1, 1, 1)$  the central cube represents a Dirac monopole with plaquette values summing up to  $2\pi$ . The link variables of the central cube correspond to an  $SU(2)$  rotation of a unit vector from one corner to the other, *i.e.*,  $\cos(\omega) = 1/3 = (-1, -1, -1)(1, -1, -1)/3$ . Due to the non-abelian nature of the  $SU(2)$  gauge field for increasing distance from the center the field strength approaches zero. No antimonopole is needed to compensate the monopole.

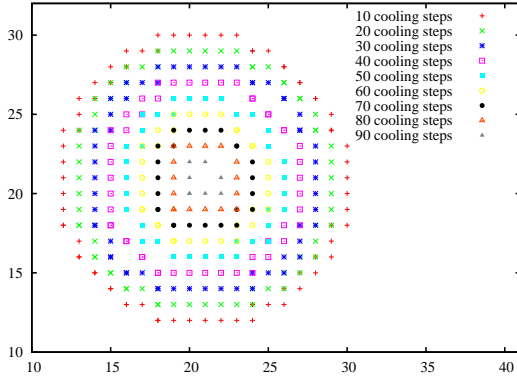


FIG. 6. Cooling of a spherical vortex with  $\alpha = \alpha_-$  on a  $40^3 \times 2$  lattice. In maximal abelian gauge a monopole-antimonopole circle shrinks and vanishes at 92 cooling steps.

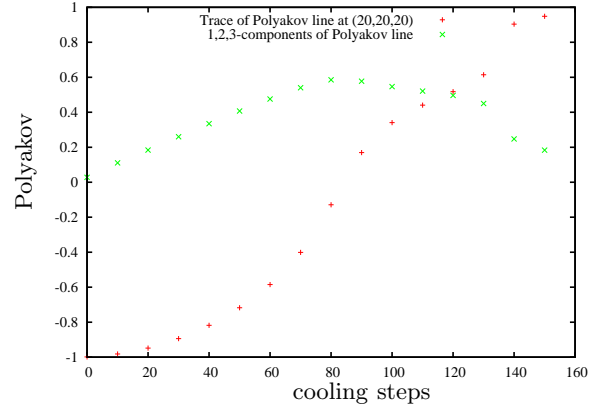


FIG. 8. Polyakov-line at special site  $(20,20,20)$  for the negative spherical vortex during cooling shows two transitions as function of the cooling step.

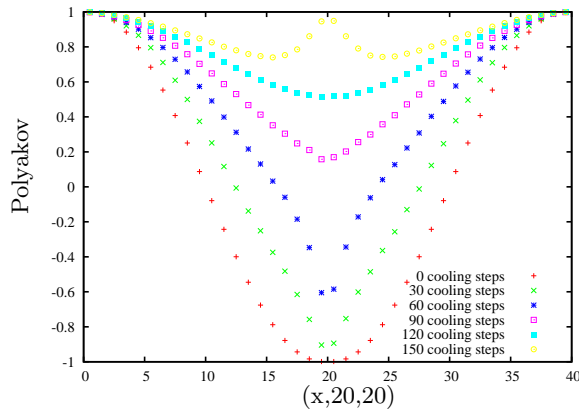


FIG. 7. Profile functions of the Polyakov loops through the lattice (varying  $x$  at  $y = 20$  and  $z = 20$ ) during cooling.

The Polyakov loops around the central cube form a hedgehog. They reflect the color directions of the link variables. A parallel-transport to the above color frame leads to parallel Polyakov lines in color direction  $(-1, -1, -1)$ . The profile function of the Polyakov loops through the lattice during cooling is shown in Fig. 7 and the course of the central Polyakov line is plotted in Fig. 8. We find two transitions, one smooth between cooling steps 70 and 90 and a jump after 130 cooling steps, where the monopole finally vanishes. The color directions of link-, plaquette- and Polyakov matrices of the central cube of the negative spherical vortex after 120 cooling steps are depicted in Fig. 9.

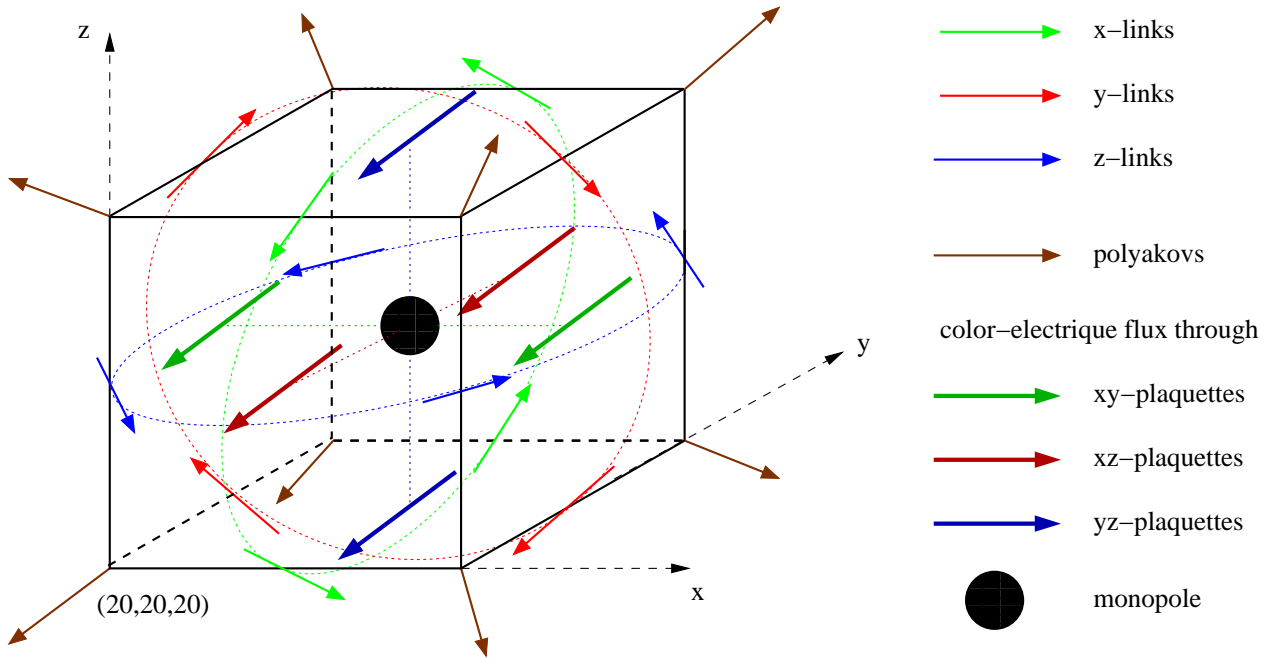


FIG. 9: The arrows indicate the rotational vectors of link-, plaquette- and Polyakov-matrices around the central cube of the negative spherical vortex after 120 cooling steps. Link-vectors rotate around the center, color fluxes through plaquettes are aligned parallel in the  $(-1, -1, -1)$ -direction and Polyakov loops form a hedgehog.

## VII. CONCLUSIONS

We reported on violations of the lattice index theorem for smooth, “admissible” gauge configurations of classical, spherical center vortices, for both, overlap and asqtad staggered fermions in the fundamental and adjoint representations. Numerically, the discrepancy equals the winding number of the spheres when they are regarded as maps  $S^3 \rightarrow SU(2)$ .

During cooling a spherical vortex on a  $40^3 \times 2$  lattice, the index in the adjoint representation indicates evidence for an object with fractional topological charge, which is identified as a Dirac monopole with the well known

singularity in its center and a gauge field fading away at large distances. Therefore even for periodic boundary conditions it does not need an antimonopole.

## ACKNOWLEDGMENTS

We thank Rob Pisarski and Jeff Greensite for the suggestion to investigate configurations with fractional topological charge with adjoint fermions. We are grateful to Mithat Ünsal and Štefan Olejník for helpful discussions. This research was partially supported by the Austrian Science Fund (“Fonds zur Förderung der Wissenschaften”, FWF) under contract P22270-N16 (R.H.).

- 
- [1] A. Casher. Chiral Symmetry Breaking in Quark Confining Theories. *Phys. Lett.*, B83:395, 1979.
  - [2] G. 't Hooft. On the phase transition towards permanent quark confinement. *Nucl. Phys.*, B138:1, 1978.
  - [3] P. Vinciarelli. Fluxon solutions in nonabelian gauge models. *Phys. Lett.*, B78:485–488, 1978.
  - [4] T. Yoneya. Z(n) topological excitations in yang-mills theories: Duality and confinement. *Nucl. Phys.*, B144:195, 1978.
  - [5] J. M. Cornwall. Quark confinement and vortices in massive gauge invariant qcd. *Nucl. Phys.*, B157:392, 1979.
  - [6] G. Mack and V. B. Petkova. Comparison of lattice gauge theories with gauge groups  $z(2)$  and  $su(2)$ . *Ann. Phys.*, 123:442, 1979.
  - [7] H. B. Nielsen and P. Olesen. A quantum liquid model for the qcd vacuum: Gauge and rotational invariance of domained and quantized homogeneous color fields. *Nucl. Phys.*, B160:380, 1979.
  - [8] H. Reinhardt and M. Engelhardt. Center vortices in continuum yang-mills theory. In *Quark Confinement and the Hadron Spectrum IV*, 2002.
  - [9] P. de Forcrand and M. D’Elia. On the relevance of center vortices to qcd. *Phys. Rev. Lett.*, 82:4582–4585, 1999.
  - [10] C. Alexandrou, P. de Forcrand, and M. D’Elia. The role of center vortices in qcd. *Nucl. Phys.*, A663:1031–1034, 2000.
  - [11] M. Engelhardt. Center vortex model for the infrared sector of yang-mills theory: Quenched dirac spectrum and chiral condensate. *Nucl. Phys.*, B638:81–110, 2002.
  - [12] R. Höllwieser, M. Faber, J. Greensite, U.M. Heller, and Š Olejník. Center Vortices and the Dirac Spectrum. *Phys. Rev.*, D78:054508, 2008.
  - [13] T. Banks and A. Casher. Chiral symmetry breaking in confining theories. *Nucl. Phys.*, B169:103, 1980.
  - [14] M. F. Atiyah and I. M. Singer. The index of elliptic operators. 5. *Annals Math.*, 93:139–149, 1971.
  - [15] A. S. Schwarz. On regular solutions of euclidean yang-mills equations. *Phys. Lett.*, B67:172–174, 1977.
  - [16] L. S. Brown, R. D. Carlitz, and C. Lee. Massless excitations in instanton fields. *Phys. Rev.*, D16:417–422, 1977.
  - [17] R. Narayanan and H. Neuberger. A construction of lattice chiral gauge theories. *Nucl. Phys.*, B443:305–385, 1995.
  - [18] G. Jordan, R. Höllwieser, M. Faber, and U.M. Heller. Tests of the lattice index theorem. *Phys. Rev.*, D77:014515, 2008.
  - [19] H. Neuberger. Exactly massless quarks on the lattice. *Phys. Lett.*, B417:141–144, 1998.
  - [20] H. Neuberger. More about exactly massless quarks on the lattice. *Phys. Lett.*, B427:353–355, 1998.
  - [21] M. Lüscher. Abelian chiral gauge theories on the lattice with exact gauge invariance. *Nucl. Phys.*, B549:295–334, 1999.
  - [22] H. Neuberger. Bounds on the wilson dirac operator. *Phys. Rev.*, D61:085015, 2000.
  - [23] H. Fukaya et al. Overlap fermion with the topology conserving gauge action. *PoS, LAT2005:123*, 2006.
  - [24] K. Y. Wong and R. M. Woloshyn. Topology and staggered fermion action improvement. *Nucl. Phys. Proc. Suppl.*, 140:620–622, 2005.
  - [25] A. Hasenfratz and F. Knechtli. Flavor symmetry and the static potential with hypercubic blocking. *Phys. Rev.*, D64:034504, 2001.
  - [26] M. Garcia-Perez, A. Gonzalez-Arroyo, and A. Sastre. Adjoint zero-modes as a tool to understand the Yang-Mills vacuum. *PoS, LAT2007:328*, 2007.
  - [27] R. G. Edwards, U. M. Heller, and R. Narayanan. Evidence for fractional topological charge in SU(2) pure Yang-Mills theory. *Nucl. Phys. Proc. Suppl.*, 73:497–499, 1999.
  - [28] T. M. W. Nye and M. A. Singer. An  $L^2$ -Index Theorem for Dirac Operators on  $S^1 * R^3$ . 2000, [arXiv:math/0009144].
  - [29] E. Poppitz and M. Ünsal. Index theorem for topological excitations on  $R^3 * S^1$  and Chern-Simons theory. *JHEP.*, 0903:027, 2009.
  - [30] T. T. Wu and C. Yang. Some Remarks About Unquantized Nonabelian Gauge Fields. *Phys. Rev.*, D12:3843–3844, 1975.
  - [31] M. Faber and A. P. Kobushkin. Electromagnetic field from the Skyrme term. *Phys. Rev.*, D69:116002, 2004.
  - [32] P. Skala, M. Faber, and M. Zach. Magnetic Monopoles and the Dual London Equation in SU(3) Lattice Gauge Theory. *Nucl. Phys.*, B494:293–311, 1997.

linkphase

